



doi:10.1016/j.gca.2003.11.020

Assaying the catalytic potential of transition metal sulfides for abiotic carbon fixation

G. D. CODY,* N. Z. BOCTOR, J. A. BRANDES, T. R. FILLEY, R. M. HAZEN, and H. S. YODER, JR.

Geophysical Laboratory, Carnegie Institution of Washington, 5251 Broad Branch NW, Washington, DC 20015, USA

(Received May 21, 2003; accepted in revised form November 17, 2003)

Abstract—A suite of nickel, cobalt, iron, copper, and zinc containing sulfides are assayed for the promotion of a model carbon fixation reaction with relevance to local reducing environments of the early Earth. The assay tests the promotion of hydrocarboxylation (the Koch reaction) wherein a carboxylic acid is synthesized via carbonyl insertion at a metal-sulfide-bound alkyl group. The experimental conditions are chosen for optimal assay, i.e., high reactant concentrations and pressures (200 MPa) to enhance chemisorption, and high temperature (250°C) to enhance reaction kinetics. All of the metal sulfides studied, with the exception CuS, promote hydrocarboxylation. Two other significant reactions involve the catalytic reduction of CO to form a surface-bound methyl group, detected after nucleophilic attack by nonane thiol to form methyl nonyl sulfide, and the formation of dinonyl sulfide via a similar reaction. Estimation of the catalytic turnover frequencies for each of the metal sulfides with respect to each of the primary reactions reveals that NiS, Ni₃S₂, and CoS perform comparably to commonly employed industrial catalysts. A positive correlation between the yield of primary product to NiS and Ni₃S₂ surface areas provides strong evidence that the reactions are surface catalytic in these cases. The sulfides FeS and Fe_(1-x)S are unique in that they exhibit evidence of extensive dissolution, thus, complicating interpretation regarding heterogeneous vs. homogeneous catalysis. With the exception of CuS, each of the metal sulfides promotes reactions that mimic key intermediate steps manifest in the mechanistic details of an important autotrophic enzyme, acetyl-CoA synthase. The relatively high temperatures chosen for assaying purposes, however, are incompatible with the accumulation of thioesters. The results of this study support the hypothesis that transition metal sulfides may have provided useful catalytic functionality for geochemical carbon fixation in a prebiotic world (at least initially) devoid of peptide-based enzymes. Copyright © 2004 Elsevier Ltd

1. INTRODUCTION AND BACKGROUND

The abiological reduction of oxidized C₁ carbon, e.g., CO₂ and/or CO, to form organic molecules was (and likely continues to be) a ubiquitous chemical process operating in many regions of the Solar System. Reduction of oxidized carbon in the presence of minerals via Fischer-Tropsch (FT) like processes (Fischer, 1935) has been proposed as a source of many of the complex organic compounds contained within carbonaceous chondrites (e.g., Hayatsu and Anders, 1981; Kress and Tielsens, 2001) as well as an abiotic source of hydrocarbons in terrestrial settings (e.g., McCollom et al., 1999; Sherwood Lollar et al., 2002). Abiotic reduction of CO₂ in terrestrial environments may have provided for the synthesis of a broad range of organic compounds early in the history of Earth and Mars (Shock et al., 1996). Ultimately, natural reactions starting with the abiotic reduction of CO₂ may have been useful for the development of more complex chemistry relevant to the emergence of life (e.g., Wächtershäuser, 1988a; Russell and Hall, 1997; Cody et al., 2001).

Fluids with hydrogen activities fixed by the oxygen buffer fayalite-magnetite-quartz (FMQ), thermodynamically favor the reduction of CO₂ to CH₄ at temperatures lower than ~400°C (see, for example, Shock, 1992; Schulte and Shock, 1993). Shock (1992) noted that if methane formation is kinetically inhibited, then the formation of various higher molecular weight organics is also exergonic. Notwithstanding these fa-

vorable thermodynamics, catalysts are required to promote such organic reactions. Industrially, the conversion of CO₂ (CO) and H₂ to high molecular weight hydrocarbons utilizes proprietary catalysts; typically metals (and minerals) containing Group VIII elements deposited on chemically inert support particles (e.g., Adamson, 1990). In natural environments, heterogeneous catalysts for CO₂ (CO) reduction are presumed to be the surfaces of certain minerals.

Reduced fluids are common in extant hydrothermal settings, for example in continental hot springs (Chapelle et al., 2002) and spreading centers in the deep ocean (see review by Holm, 1992). The mineralogy associated with such fluids is often rich in various transition metal sulfides including chalcopyrite (CuFeS₂), pyrite (FeS₂), sphalerite (ZnS), and pyrrhotite (Fe_{1-x}S) (e.g., Tivey, 1995). It has been proposed by Wächtershäuser (1988a) that certain transition metal sulfides, in particular pyrrhotite and pyrite, in the presence of reduced fluids may promote abiotic organic reactions of relevance to origins of life chemistry. Russell et al. (1998) favor the specific sulfide phases mackinawite [Fe(Ni,Co)_{1+x}S], greigite (Fe₃S₄), and violarite (FeNi₂S₄) as potentially important prebiotic catalysts.

In apparent support of these ideas are the results of experiments that suggest promoting (possibly catalytic) qualities of transition metal sulfides in certain important organo-synthetic reactions. For example, Heinen and Lauwers (1996) demonstrated the reduction of CO to form methane thiol (CH₃SH), and other alkane thiols, in the presence of pyrrhotite and H₂S at temperatures of 100°C. In these experiments, the oxidation of pyrrhotite to form pyrite was presumed to be the source of reducing power (see, for example, Hall, 1986; Wächtershäuser,

* Author to whom correspondence should be addressed (g.cody@gl.ciw.edu).

Table 1. Metal sulfides, reaction conditions, reagent concentrations, and surface areas.

Mineral	Time (h)	T (°C)	P (MPa)	ρ (g/cm ³)	Mean part. radius (μ m)	Wt. mineral in reactor (mg)	Nonane thiol (μ mol)	HCOOH (μ mol)	H ₂ O (μ mol)	Total mineral area (cm ²)
Ni-metal	6	250	200	8.9	9.5	15.0	30.9	109.0	34.4	5.3
NiS	6	250	200	5.5	8.1	15.3	30.6	93.5	29.5	10.3
NiS	1	250	200	5.5	8.1	15.2	29.6	108.0	34.1	10.2
CoS	6	250	200	5.45	10.3	15.1	27.6	95.0	30.0	8.1
CoS	1	250	200	5.45	10.3	14.6	25.6	115.5	36.5	7.8
Ni ₃ S ₂	6	250	200	5.82	6.4	14.8	28.8	92.5	29.2	12.0
Ni ₃ S ₂	6	250	200	5.82	6.4	5.0	30.5	81.4	25.7	4.1
Fe _{1-x} S	6	250	200	4.58–4.65	8.9	14.7	33.2	134.9	42.6	10.7
Fe _{1-x} S	1	250	200	4.58–4.65	8.9	15.0	29.8	105.8	33.4	10.9
FeS	6	250	200	4.6	13.8	15.3	32.4	108.5	34.2	7.2
FeS ₂	6	250	200	5.02	10.1	15.4	23.9	110.7	35.0	9.1
(Fe,Ni) ₉ S ₈	6	250	200	4.6–5.0	6.7	15.6	35.5	114.9	36.3	14.6
CuFeS ₂	6	250	200	4.1–4.3	5.4	10.1	27.3	62.1	19.6	13.4
Cu ₅ FeS ₄	6	250	200	5.06–5.08	8.2	10.0	26.3	63.8	20.2	7.2
CuS	6	250	200	4.6–4.76	9.2	15.7	28.6	110.3	34.8	10.9
Cu ₂ S	6	250	200	5.5–5.8	17.3	15.0	32.1	109.9	34.7	4.6
ZnS	6	250	200	3.9–4.1	4.1	15.4	38.6	116.5	36.8	28.2
Blank	6	250	200	—	—	—	30.1	107.2	33.8	—

1988b). Whether formation of methane thiol occurred on the surface of pyrrhotite or pyrite was not established.

In 1997, Huber and Wächtershäuser reported a high conversion of methane thiol to acetic acid in the presence of both CO and a mixed Ni- and Fe-containing sulfide precipitate formed from an aqueous reaction of Na₂S with FeSO₄ · 7H₂O and NiSO₄ · 6H₂O. They proposed that the reaction was catalyzed on the surface of an ordered (Ni,Fe)S precipitate, following a mechanism similar to that proposed for methanol carbonylation to acetic acid by CO in the presence of a cobalt catalyst.

The original methanol-to-acetate reaction employed CoI₂ as a catalyst precursor (see discussion in Cotton and Wilkinson, 1988). The key step involves the conversion of methanol to methyl iodide coupled with carbonylation of CoI₂; the similarity in the roles of iodide ion and bisulfide ion as effective leaving groups suggest similarity in mechanism between the Huber and Wächtershäuser (1997) reaction and the methanol-to-acetate reaction (Crabtree, 1997). What is not clear, however, is whether or not the reaction reported by Huber and Wächtershäuser (1997) was catalyzed heterogeneously on the surface of a sulfide precipitate or homogeneously via organo-metallic complexes in solution.

The distinction between hetero (surface)- and homo (solution)-catalytic processes is important. One of the central postulates of Wächtershäuser's "Iron-Sulfur World" theory is that pyrite surfaces catalyze reactions. If the fundamental anabolic (carbon-carbon bond forming) reactions described above occurred in solution catalyzed by soluble metal complexes, then such reactions in solution are subject to the probability of favorable reactant collision; under dilute conditions the probability of profitable collisions is small. If, however, mineral surfaces scavenge dilute solutions for reactants through favorable adsorption characteristics, then surface adsorption can lead to an enormous rate enhancement of bimolecular and higher-order reactions by virtue of increasing the effective molarity of reactants (e.g., Abeles et al., 1992). Catalytic minerals can exhibit similar concentration-enhancing qualities as do en-

zymes (e.g., Schoonen et al., 1998). Reaction rates may be further enhanced by chemisorption that weakens strong covalent bonds, further accelerating reaction kinetics.

The goal of the present research is to both assay the promoting qualities of a number of transition metal sulfides (including pyrite) for potentially useful primitive carbon fixation chemistry, as well as to ascertain evidence, if any, for surface catalytic mechanisms of reaction.

2. EXPERIMENTAL

2.1. Metal Sulfide Synthesis and Characterization

Natural metal sulfides rarely are compositionally pure, rather extensive cationic substitution is often encountered. Even a minor amount of substitution, e.g., Ni²⁺ for Fe²⁺ in FeS or Mn²⁺ for Zn²⁺ in ZnS, may affect significant changes in catalytic properties. Although the effects of such substitutions should be studied in the future, it was felt that, as an initiation point, working with compositionally pure mineral sulfide phases would provide a better base line for the intrinsic catalytic qualities of simple metal sulfides. Consequently, the mineral phases explored in this study, were synthesized, dry, from puratronic-grade metals (99.995–99.998%) and S (99.9995%) with standard, solid-state procedures (Kullerud, 1971). At the termination of the synthesis, a small portion of each charge is mounted in epoxy, polished with diamond abrasive paste, and examined optically in reflected light to ensure that the target phase is the only phase present. The chemical compositions of the synthetic sulfides are determined by electron microprobe analysis with a JEOL Superprobe (JXA-8800). In some cases the crystal structure of the target phase was confirmed with X-ray diffraction (Cody et al., 2000). The number-averaged particle diameter was determined with optical microscopy, digital image acquisition, and particle analysis software (NIH image). The average particle radii and estimated surface areas derived from the particle size analysis are presented in Table 1.

The synthesized sulfides were stored in an evacuated desiccator until use. Care was taken to minimize the exposure of these sulfides to atmospheric oxygen and moisture; nevertheless, it is likely that some degree of surface oxidation will have occurred (e.g., Guevremont et al., 1998). Surface oxidation may influence the catalytic qualities of the mineral sulfides used in the experiments. Adding to the complexity is the possibility that the high fH_2 employed in the assay may partially reduce the mineral surfaces. In either case, it is clear that the surface

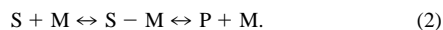
chemistry of each mineral sulfide will be a complex function of the local surface structure, as well of the precise processing/handling conditions. In the present experiments each mineral sulfide has been processed and reacted under identical conditions; thus a reasonable basis for comparison exists, subject to the caveats mentioned above.

2.2. Assay Protocol

As the central goal of this study is to test the property of various metal sulfide surfaces toward promoting the catalysis of organic reactions, it is worthwhile to recall the assaying of enzymes. Typically the catalytic activity of peptide enzymes is analyzed as a function of substrate (or reactant) concentration. Depending on the reaction mechanism, these data are then fit to an appropriate form of a Michaelis-Menten rate expression to derive the various kinetic parameters. Given the difficult nature of the present experiments (e.g., multiple sulfides, high pressures, and small reactor volumes) such experiments are prohibitive. The most straightforward method for assaying the catalytic performance of enzymes is to adopt conditions where the catalytic sites are saturated with a large excess of reactant (see, for example, Abeles et al., 1992); in other words, choose conditions that exceed the asymptotic limit of reactant concentration on reaction rate. Under these conditions (for a simple enzymatic reaction) the reaction rate is zeroth order with respect to the reactant, and is given simply as

$$R = k_{\text{cat}}[E] \quad (1)$$

where k_{cat} is the rate of the product-forming step, and $[E]$ is the concentration of the enzyme. The same requirements are necessary for assaying the catalytic performance of mineral or free-metal surfaces. For example, in the case of the simplest surface-catalyzed reaction yielding a product, P, the key steps involve substrate S adsorption on the mineral surface, M, followed by reaction and desorption e.g.,



Surface coverage, θ , of the catalyst surface is assumed to be governed by some sort of adsorption isotherm, e.g., a Langmuir isotherm where

$$\theta = K_{\text{ads}}[S]/(1 + K_{\text{ads}}[S]) \quad (3)$$

and K_{ads} is the Langmuir sorption constant. Note, also that although a given solid catalyst will have a total surface area A, the actual reactive surface area, A_o , is most likely a small fraction of A (e.g., Steinfeld et al., 1989). In other words, not all of the surface is catalytic. The rate of reaction 2 is then given as (Boudart and Djéga-Mariadassou, 1984; Schoonen et al., 1998),

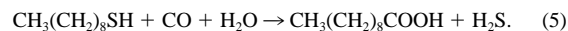
$$dS/dT = -k_{\text{cat}} \cdot A_o. \quad (4)$$

For surface-catalyzed reactions, therefore, the reaction rate is a function of k_{cat} , surface coverage, θ , and the total reactive surface area, A_o . Ideally, the experimental conditions chosen should exceed the saturation point of each mineral's surface active sites, so that one can compare the catalytic performance of each mineral as a function of the product kA_o . In the present experiments substrate concentrations are in far excess of what would be required to provide a monolayer of coverage, i.e., 2000 to 10,000 times the estimated total mineral surface area. Furthermore, given that the reactive surface area, A_o , is likely to be a fraction of the total surface area, the actual ratio of substrate to active sites is likely to be in considerable excess of a factor of 10,000.

In addition to the high substrate concentrations, high pressures (200 MPa) were employed in order to favor adsorption and saturation of all of the mineral's active sites. It is recognized that the experimental conditions chosen only coarsely mimic the chemistry of crustal or deep oceanic hydrothermal vent environments. For the purpose of deriving a comparative assessment of potential promoting activity across a range of mineral sulfides, however, the selected experimental conditions do provide a useful assay.

The assay reaction chosen as a model for simple carbon fixation is the hydrocarboxylation/hydrocarbonylation reaction (the Koch reaction; see March, 1991). In such a reaction, a carbonyl insertion at a chemisorbed alkyl group on the catalyst surface, leads to a catalyst bound alkyl group that, when attacked by hydroxide or bisulfide,

yields a carboxylic acid or thioacid, respectively. The chosen substrate was nonane thiol ($C_9H_{19}SH$) and the source of CO was aqueous formic acid. Reaction conditions were 200 MPa and 250°C for a duration of 6 hs. The temperature of 250°C was chosen both to favor formic acid decomposition to predominantly CO_2 and H_2 (however, some CO and water will be formed via the water-gas shift reaction, WGS; McCollom et al., 1999), as well as to enhance the overall reaction rate. Simplified, the target reaction is written as



The choice of nonane thiol (e.g., over methane thiol) was purely for practical reasons; nonane thiol is relatively nonvolatile, thus enhancing quantitative recovery. Furthermore, the low volatility of nonane thiol ensured a lower stench hazard should an experiment have failed. Aqueous formic acid was chosen as a practical means of adding stoichiometric CO_2 , CO, H_2O , and H_2 to the relatively small reactors. In some cases ^{13}C labeled formic acid was used in order to prove that carbon additions were unambiguously derived from formic acid.

The choice of reactor requires special consideration when exploring surface catalytic reactions. Given the high pressures used in the present experiments, pure gold tubes were chosen while recognizing that it is well known that organothiols readily thiolate gold surfaces (Bain et al., 1989). The extent to which thiolation of the reactor surfaces occurred in the experiments was not determined; but analysis of blank (mineral absent) runs revealed no evidence of any reaction other than the thermal condensation of nonane thiol to form dinonyl disulfide and H_2 . This test implies that any reaction that may have occurred between the substrates and the reactor surface did not affect the outcome of the assay reaction.

2.3. Sample Handling and Analysis

Prior to use, the 2.4 mm outer diameter, gold-tube reactors are refluxed sequentially in hydrochloric acid and nitric acid and then annealed at 900°C. Prior to sealing, the tubes were blanketed with dry N_2 , immersed in liquid N_2 , and arc welded. All reactors were weighed both before and after each experimental run in order to test for leakage. Yoder (1950) has previously described the gas-media apparatus used to achieve the high pressures and temperatures. In brief, argon-gas pressures up to 200 MPa are generated with a gas compressor, whereas pressures above 200 MPa require a second-stage intensifier. Pressure was measured resistively to within ± 10 kPa with a calibrated manganin-wire coil. A given reaction temperature was achieved with a long, platinum-wound furnace mounted on a thin-walled mullite tube, with continuous monitoring for the duration of each experiment. The temperature variation is precise to within $\pm 0.1^\circ C$ and accurate to within $\pm 0.3^\circ C$.

Immediately prior to analysis, each gold tube reactor was immersed in liquid nitrogen to freeze the volatiles, particularly CO_2 . Each reactor was opened at both ends and transferred to a 4-dram vial. Approximately 1 mg of pentadecane was weighed into each sample vial as a concentration standard. All organic acids were converted to their volatile propyl esters with a solution of 14% (vol) BF_3 -propanol complex in propanol at 90°C with standard esterification procedures (e.g., Blau and King, 1977). Analysis of the esterified products was performed with gas chromatography-mass spectrometry with a Hewlett-Packard 6890 Series gas chromatograph interfaced to a 5972 Series mass selective detector. Product concentrations were obtained from the total ion current with calibration curves from which the response factors of the compounds had been previously determined with pure standards. In the case of the few compounds unavailable commercially, response factors were assumed to be equal to that of the standard.

Chromatography was performed with a 14% cyanopropyl-86% dimethyl-silicone capillary column. Identification of unknown compounds relied on the interpretation of fragmentation behavior with both electron-impact and chemical-ionization mass spectrometry; the latter method employed either methane or isobutane as the ionization gas. The product compounds and their characteristic fragment ions are listed in the Appendix. Details of the reactions, concentrations of metal sulfide and organic reactants, and reaction conditions are presented in Table 1.

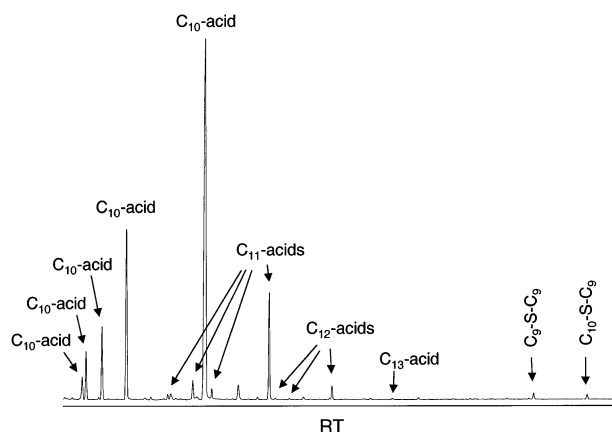


Fig. 1. Chromatogram of the products from the reaction of nonane thiol and aqueous formic acid over Ni^0 . Reaction conditions were 200 MPa, 250°C, and 6 h. Peak intensity is given by the total ion current (TIC) monitored at the electron multiplier of the mass spectrometer and plotted against retention time (RT). The peaks labeled C10 correspond to isomers of propyl decanoate. Peaks labeled C11, C12, and C13 refer to esterified isomers of C + 2, C + 3, and C + 4 carbon additions to a metal bound nonyl group. Dinonyl sulfide and nonyl decyl sulfide are the only sulfur-containing species observed in the reactions over Ni^0 .

3. RESULTS AND DISCUSSION

3.1. Practical Issues with Mineral Catalyzed Organic Reactions

The assay reaction chosen (Eqn. 5) appears straightforward; however, as is commonly the case, multiple, competing reaction pathways may complicate the product suite. Such competition is exemplified in the products of a reaction between nonane thiol and aqueous formic acid in the presence of Ni metal particles (Figure 1), where a number of reactions lead to a broad suite of products. For example, when nonane thiol encounters the Ni^0 surface, an elimination reaction is possible, yielding 1-nonene and H_2S (or more likely the sulfidization of the Ni^0 with the production of H_2). Given the strong thermodynamic driving force to sulfidize Ni^0 , virtually all of the nonane thiol and H_2S (and HS^-) is consumed from the solution and the majority of products (Fig. 1) are not sulfur-containing. An exception is a pair of organomonosulfides: dinonyl sulfide and nonyl-decyl sulfide as seen to the right in Figure 1.

Evidence for the rapid desulfurization of nonane thiol preceding carbonyl insertion is clearly seen in the broad range of C10 carboxylic acids formed. Previous data derived for the reaction 1-nonene and formic acid over NiS catalyst (Cody et al., 2001) revealed a broad distribution of C10 acids which was

Table 2. Organic products identified in reactions of formic acid and nonane thiol at 250°C and 200 MPa for 6 h.^a

Organic compounds	Ni metal	Ni_3S_2	NiS	CoS	FeS	CuS	Cu_2S	CuFeS_2	Cu_5FeS_4	FeS_2	$(\text{Fe},\text{Ni})_9\text{S}_8$	ZnS	Blank
2-Nonane thiol ^b			+										
1-Nonane thiol (reactant)			+	+	+		+	+	+	+	+	+	+
1-Decanoic acid (target)	+	+	+	+	+		+	+	+	+	+	+	
2-Methyl nonanoic acid	+	+	+	+									
2-Ethyl octanoic acid	+	+	+	+									
2-Propyl heptanoic acid	+	+	+	+									
2-Butyl hexanoic acid	+	+	+	+									
2-Pentyl thiophene		+	+	+	+				+			+	
Methyl 1-nonyl sulfide		+	+	+	+	+	+	+	+	+	+	+	
Methyl 2-nonyl sulfide		+	+	+			+	+				+	
Methyl 1-undecanoate		+	+	+				+	+	+	+	+	
Methyl 2-undecanoate		+	+	+				+	+	+	+	+	
Methyl 1-nonyl disulfide				+	+	+		+	+	+	+	+	
1-Methylthio-2-nonane thiol					+								
1-Undecanoic acid	+	+	+	+									
3-Methyl decanoic acid	+	+	+	+									
3-Ethyl nonanoic acid	+		+	+									
3-Propyl octanoic acid	+		+	+									
3-Butyl heptanoic acid	+		+	+									
1-Dodecanoic acid	+												
4-Methyl undecanoic acid	+												
4-Ethyl decanoic acid	+												
4-Propyl nonanoic acid	+												
4-Butyl octanoic acid	+												
1-Tridecanoic acid	+												
1,1' Dinonyl sulfide	+ ^c	+	+	+	+	+	+	+	+	+	+	+	
1,1' Decyl nonyl sulfide	+	+	+	+			+	+		+			
1,1' Dinonyl disulfide		+	+	+	+	+	+	+	+	+	+	+	+
1,1' Decyl nonyl disulfide		+	+	+			+			+			
1-Methylthio-2-nonylthio-nonane		+ ^d			+							+	
1-Propylthio-2-nonylthio-nonane			+	+	+		+	+	+	+	+	+	
1,1' Dinonyl trisulfide					+								

^a +, present.

^b Also present are the 3-, 4-, and 5- isomers.

^c Also present other positional isomers.

^d Propyl group from derivatization.

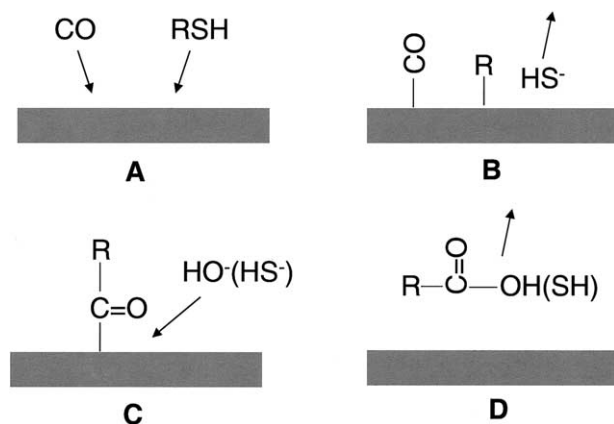


Fig. 2. Depiction of a surface promoted carbonyl insertion leading to the principal assay product, decanoic acid. In the first step (A), the metal sulfide surface is carbonylated by chemisorption of CO. Nonane thiol then alkylates the surface (B), liberating bisulfide. Surface diffusion brings the CO group in proximity to the metal bound nonyl group. Carbonyl insertion (C), leads to the formation of a metal bound decanoyl group. Nucleophilic attack (D) by either hydroxyl or bisulfide hydrolyzes the decanoyl group forming decanoic acid or thioacid.

indicative of extensive double-bond migration along the nonene carbon skeleton prior to CO insertion (i.e., the oxo reaction, March, 1991). In the case of the Ni^0 reaction groups of C11, C12, and C13 carboxylic acid isomers are also present in the product suite (Fig. 1), revealing that following carbonyl insertion, reduction of the carbonyl function is possible, followed by further carbonyl insertions. If this sequence of steps is not terminated by hydrolysis, C11, C12, and higher acid products will form (e.g., Figure 1). The final product suite is the result of a kinetic competition among the most facile chemical reaction pathways (Appendix). The overall final distribution results from a situation wherein the surface hydrolysis rate (forming terminal acids or thioacids) is comparable to that of carbonyl reduction. The important point is that even given a rather simple reaction, e.g., Eqn. 5, a broad range of products resulting from competitive side reactions may also be expected.

Similarly, the products derived from reactions over transition metal sulfides reveal a broad range of compounds that are also derived from a kinetic competition between reactions (note, however, that these products are different from those formed over Ni^0 ; see Table 2). Reactions in the presence of Ni_3S_2 , NiS, and CoS exhibit only a trace of the carboxylic acid isomer products that were predominant in the analogous reaction over Ni^0 (e.g., C11, C12, and higher carboxylic acid isomers). The principal products of the reactions in the presence of the various mineral sulfides studied reveal a predominance of disulfides (formed via the condensation of thiols to liberate H_2), alkyl sulfides (formed from surface bound alkyl groups reacting with thiols), and the assay target compound, 1-decanoic acid.

3.2. Assay of Transition Metal Sulfides and Related Reactions

Starting with the presumption that the assay reaction (Eqn. 5) is heterocatalytic, one can envision the surface mechanism as diagrammed in Figure 2. The sequence of the reaction starts with

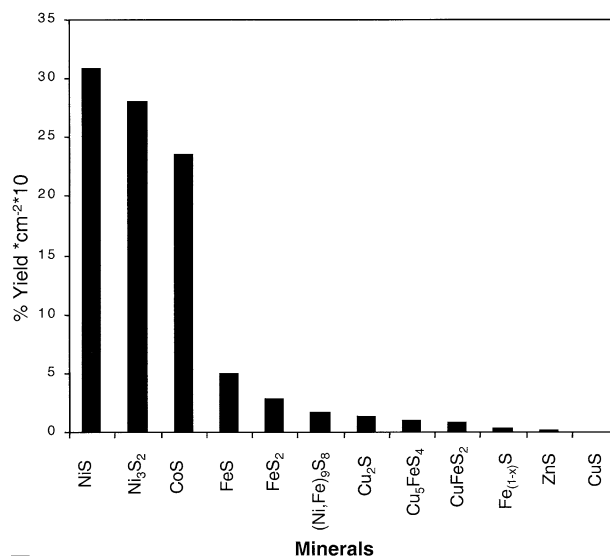


Fig. 3. Yield of decanoic acid (detected as propyl decanoate) normalized to surface area of the metal sulfide. Note that with exception of CuS and the blank (not shown), each metal sulfide promoted some reaction. Reaction conditions were 200 MPa, 250°C, and 6 h.

carbon monoxide carbonylating exposed metal atoms on the mineral surface (Fig. 2A); nonane thiol then chemisorbs to the mineral surface eliminating bisulfide ion back to the solution (Fig. 2B). Surface migration of the CO group and insertion into the alkyl-metal bond leads to the formation of a decanoyl-metal intermediate (Fig. 2C). Nucleophilic attack of the decanoyl-metal bond by either a solution hydroxyl or bisulfide ion results in the liberation of either decanoic acid or decanoic thioacid into the solution, and, thus, frees the catalytic site to interact with fresh substrate (Fig. 2D).

If it is presumed that the transition metal sulfides investigated in the present study are operating entirely heterocatalytically, then the only valid means of comparing the relative performances of each of the metal sulfides is to rank the yield of product normalized to the total surface area. These data are shown in Figure 3. The top performers on this basis are NiS, Ni_3S_2 , and CoS; an expected conclusion since it is well known that Group VIII elements generally provide the best catalytic enhancement of the Koch and related reactions (Cotton and Wilkinson, 1988). Note that although the nickel-bearing phases are the top performers, this does not mean that the presence of nickel alone ensures enhanced catalytic performance. Pentlandite, $(\text{Ni,Fe})_9\text{S}_8$, for example, contains 50% nickel yet its apparent performance is less than that of some pure iron-containing phases, e.g., troilite (FeS) and pyrite (FeS₂) (Fig. 3). What is somewhat surprising is that all but one of the metal sulfides studied promote the Koch reaction to a small extent, the only exceptions being covellite (CuS) and the blank (metal sulfide free). There is no evidence that copper (II) can form a bond with carbon (Cotton and Wilkinson, 1988); therefore, it is not expected that covellite (CuS) would be capable of promoting the Koch reaction.

A side significant side reaction in these reactions results in the formation of methyl nonyl sulfide (Table 2). The use of ¹³C-labeled formic acid reveals that the methyl group in this

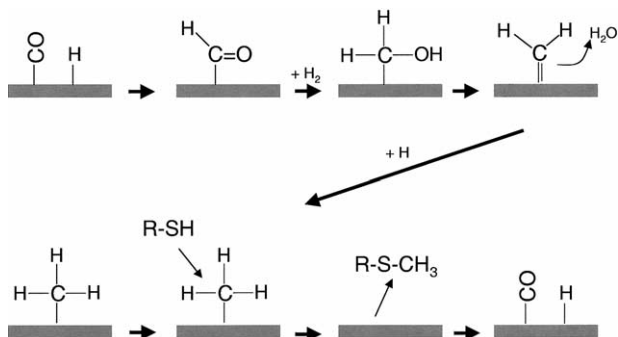


Fig. 4. Depiction of a surface promoted reduction of CO leading to a surface bound methyl group. Nucleophilic attack of the surface bound methyl group by nonane thiol yields methyl nonyl sulfide.

compound is derived from the reduction of CO derived from formic acid. Mechanistically, the reduction of CO is the first step in the Fischer-Tropsch process (Fischer, 1935). A diagram highlighting one possible route for the surface catalytic synthesis of methyl nonyl sulfide is presented in Figure 4. Progressive reduction of surface bound CO leads to the surface-bound methyl group. Nucleophilic attack of the metal-bound methyl group by nonane thiol leads to the formation of methyl nonyl sulfide.

The yield of methyl nonyl sulfide in the presence of each of the metal sulfides is presented in Figure 5, normalized to the total surface area and arranged in the same order as in Figure 3. All of the metal sulfides promoted some reduction of CO to form methyl groups and ultimately, methyl nonyl sulfide. No methyl nonyl sulfide is detected in the absence of mineral sulfide. The top performer for the production methyl nonyl sulfide is the copper (I) sulfide, chalcocite (Cu_2S).

Interestingly, covellite (CuS), although incapable of promoting the Koch reaction (Fig. 3), is a respectable promoter of the CO reduction reaction (Figure 5). This is surprising and suggests that some degree of reduction of surface Cu(II) to Cu(I) must have occurred, thus enabling the promotion of CO reduc-

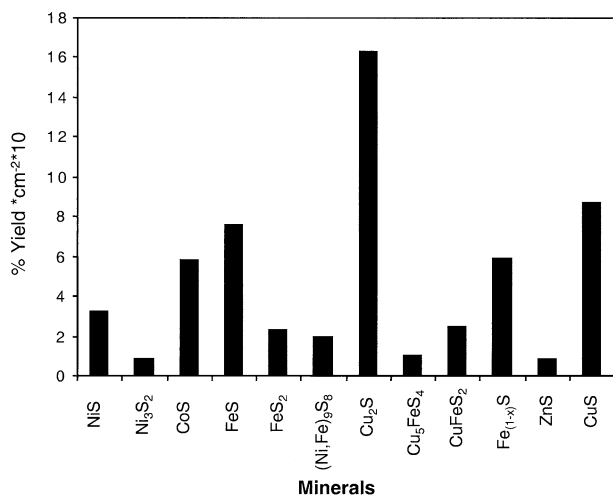


Fig. 5. Yield of methyl nonyl sulfide normalized to metal sulfide surface area for the suite of metal sulfides investigated.

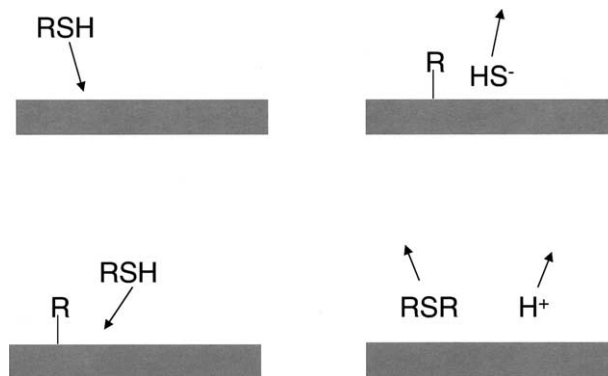


Fig. 6. Depiction of a surface promoted synthesis of dinonyl sulfide. Following nonylation of the metal sulfide surface, nucleophilic attack of the nonyl metal sulfide bond by nonane thiol yields dinonyl sulfide.

tion, but not promotion of the Koch reaction. Although many of the metal sulfides are active promoters of CO reduction, few promote the reduction of the decanoyl intermediate to form high molecular weight products (evident as C11, C12, and C13 carboxylic acids, as in the case of the Ni^0 -promoted reactions) (Fig. 1, Table 2).

A second significant side reaction promoted in the presence of mineral sulfides is the formation of dinonyl sulfide formed through alkylation of the mineral surfaces followed by attack of the nonyl-metal bond by nonane thiol to form free dinonyl sulfide (see Fig. 6 for diagram of such a surface reaction). The relative yield of dinonyl sulfide (again normalized to total surface area) is intriguing (Fig. 7). It might be expected that promotion of this reaction would correlate positively with decanoic acid yield (Fig. 3), i.e., promotion of the Koch reaction would clearly be favored by enhanced nonylation of the metal sulfide surface. In the case of NiS and CoS, such a correlation is apparent. However, in the case of the sulfide, Ni_3S_2 , evidently an excellent Koch reaction catalyst, relatively mediocre promotion of the dinonyl sulfide reaction is observed.

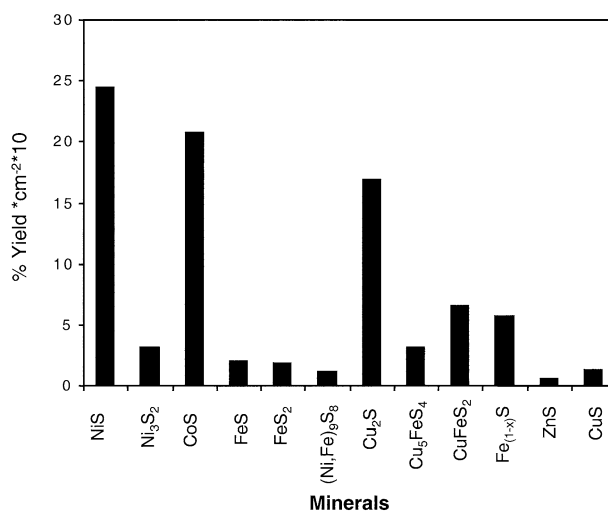


Fig. 7. Yield of dinonyl sulfide normalized to metal sulfide surface area for the suite of metal sulfides investigated.

Table 3. Yields of major acid and alkyl sulfide products.

Mineral	Nonane thiol (μmol)	C10 Acid (μmol)	Yield C10 acid (%)	CH ₃ -S-R ^a (μmol)	Yield CH ₃ -S-R (%)	R-S-R (μmol)	Yield R-S-R (%)	No. of catalytic sites (nmol) ^b	No. of turnovers C10 acid	No. of turnovers CH ₃ -S-R	No. of turnovers R-S-R
Ni-metal	30.9	16.6 ^c	53.7	ND	—	0.4	1.4	3.5	4716	—	— ^d
NiS	30.6	9.7	31.6	1.0	3.4	7.7	25.2	6.8	1426	151	1132
Ni ₃ S ₂	28.8	9.7	33.7	0.3	1.0	1.1	3.8	7.9	1227	38	139
CoS	27.6	4.9	17.8	1.2	4.3	4.3	15.6	5.4	907	222	796
FeS	32.4	1.0	3.1	1.5	4.6	0.4	1.2	4.1	244	366	98
FeS ₂	23.9	0.6	2.5	0.5	2.1	0.4	1.7	6.0	100	417	67
(Fe,Ni) ₉ S ₈	35.5	0.9	2.5	1.0	2.8	0.6	1.7	9.7	93	103	62
Cu ₂ S	32.1	0.2	0.6	2.4	7.5	2.5	7.8	3.0	67	800	833
Cu ₅ FeS ₄	26.3	0.2	0.8	0.2	0.8	0.6	2.3	4.7	43	43	128
CuFeS ₂	27.3	0.3	1.1	0.9	3.3	2.4	8.8	8.9	34	101	270
Fe _(1-x) S	33.2	0.1	0.3	2.1	6.3	2.0	6.0	7.1	14	296	282
ZnS	38.6	0.1	0.3	0.9	2.3	0.6	1.6	18.7	5	48	32
CuS	28.6	ND	—	2.7	9.4	0.4	1.4	7.2	—	375	56
Blank	30.1	ND	—	ND	—	—	—	—	—	—	—

^a R = CH₃(CH₂)₈.

^b Calculated from estimated surface assuming reactive molecular surface area for reaction is 25 Å².

^c The total yield of acids does not include the C₁₁, C₁₂, and C₁₃ acids also present in the Ni⁰ runs.

^d Due to the high degree of desulfurization of nonane thiol in the presence of Ni⁰, any turnover derived from thioether yield is not representative of catalytic quality.

Chalcocite (Cu₂S), on the other hand, exhibits both favorable kinetics for the formation of dinonyl sulfide and CO reduction implying facile carbonylation and nonylation of its surface, yet minimal yield of decanoic acid indicates minimal carbonyl insertion.

Examples such as Ni₃S₂ and Cu₂S reveal that the chemistry occurring on the surfaces of the various mineral sulfides is considerably more complex than that diagramed in Figures 2, 4, and 6. For example, NiS and Ni₃S₂ exhibit nearly identical Koch reaction yields (Fig. 3), but exhibit significantly different yields of the side product methyl nonyl sulfide and dinonyl sulfide (Figs. 5 and 7). Such differences highlight the hidden complexity of the mineral sulfide surface chemistry and suggests that there likely exists a variety of reactive centers distributed across the mineral surfaces and that promote different reaction pathways (Boudart and Djéga-Mariadassou, 1984).

3.3. Are the Koch and Other Reactions Surface Catalyzed?

Up to this point the reactions described have been presumed to be entirely surface catalytic, i.e., the reactions are promoted by substrate interactions on the surface of the metal sulfides (Figs. 2, 4, and 6). Given this assumption, it is reasonable, therefore, to consider how many turnovers occurred during the duration of the experiment, i.e., how many times did the reactants saturate the active surface sites, react and then leave the surface, thus freeing up sites for additional reactant binding.

To estimate the turnover numbers some assumptions are required. First, as the fraction of catalytically active surface relative to the total surface is unknown, it is assumed that the total mineral surface area is reactive. Second, it is assumed that the number of surface sites is equal to the total surface area divided by the estimated area of the chemisorbed reactant molecule. Estimates of the area of a chemisorbed fatty acid are on the order of 2.5 nm² (Adamson, 1990); it is assumed here that this area is also a reasonable estimate for the coverage of

an individual decanoyl group decorating the catalyst surface. In Table 3 the estimated number of catalytic sites and corresponding number of turnovers are presented for each mineral sulfide for each of the major reactions (Figs. 2, 4, and 6).

It is important to reiterate that the active surface area is likely to only be a small fraction of the total surface area and, therefore, the estimated number of turnovers presented in Table 3 provides a minimum estimate. The turnover frequency is then estimated by dividing the number of turnovers by the reaction time. For example in the case of NiS, the minimum turnover frequency is 4 min⁻¹. For comparison the turnover frequency (ν) for dinitrogen reduction to ammonia over iron is on the order of 2 min⁻¹ (Boudart and Djéga-Mariadassou, 1984); for the hydrogenation of ethylene over platinum ν is ~1.5 min⁻¹ (Boudart and Djéga-Mariadassou, 1984); and for the methanation of carbon monoxide over Co⁰, ν is ~12 min⁻¹ (Adamson, 1990).

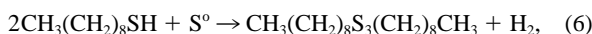
If the reactions described above are truly surface catalytic then the yield of decanoic acid should correlate with the total surface area, all other things remaining equal. To explore this relationship a series of reactions were run over NiS with a range of catalytic surface areas (0.14–3.5 cm², Table 4). Also, two reactions involving Ni₃S₂ with different surface areas were investigated. A positive correlation of 1-decanoic acid yield with NiS (and Ni₃S₂) catalytic surface area is observed, consistent with a surface catalyzed reaction (Fig. 8). A surface catalyzed reaction may not be true, however, for all of the transition metal sulfides considered in this study.

In all cases but two, the solutions collected from the reactors after reaction involving the metal sulfides were colorless. The exceptions were FeS and Fe_{1-x}S, wherein the post-reaction solutions were colored a deep orange-red. Analysis of these solutions using UV-visible light and Raman-spectroscopy revealed the presence of carbonylated iron-sulfur species (Cody et al., 2000). The sulfides FeS and Fe_{1-x}S were also exceptional in that their presence significant quantities of dinonyl

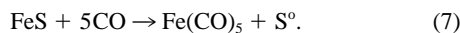
Table 4. Conversion of nonane thiol to decanoic acid as a function of surface area, 250°C, 200 MPa, 6 hs., nonane thiol + formic acid + NiS.

Sample	NiS (mg)	Mean grain size (μm)	Surface area (cm^2)	Nonane thiol(i) (μmol)	1-Decanoic acid (μmol)	Conversion (%)
1	5.19	204	0.14	29.13	0.83	2.8
2	4.95	97	0.28	29.13	1.62	5.6
3	14.92	97	0.84	31.43	2.94	9.4
4	4.96	24	1.15	32.10	2.17	6.7
5	14.90	69	1.18	41.30	4.40	10.7
6	15.23	43	1.96	31.40	2.46	7.8
7	15.05	24	3.49	24.31	2.82	11.6

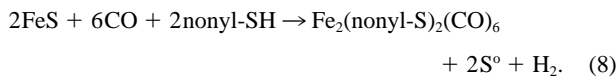
trisulfide was formed (Table 2). The synthesis of dinonyl trisulfide indicates the presence of S° in the system, for example,



where S° is derived from the Red-Ox disproportionation of FeS in the presence of CO yielding iron pentacarbonyl via reaction 7,



The source of the solution phase carbonylated iron-sulfur species is likely derived from the reaction of iron pentacarbonyl with nonane thiol or a concerted reaction involving CO, nonane thiol, and FeS (Abel and Crosse, 1967), for example,



As a consequence of reactions 6–8, solution phase carbonylated iron-sulfur species are generated in abundance (Cody et al., 2000). It is not clear in the case of troilite (FeS) and pyrrhotite (Fe_{1-x}S), therefore, whether the Koch and other

reactions were actually surface catalyzed. It is entirely possible that soluble organometallic species promoted the observed reactions. Interestingly, a trace of pyruvic acid was identified in the products of the FeS-containing reactions and was interpreted to have formed via a reaction(s) involving the carbonylated iron-sulfur solution-phase species (Cody et al., 2000).

Notwithstanding these observations, it is noted that none of the other transition metal sulfides (including the other iron-bearing phases such as pentlandite $[(\text{Fe},\text{Ni})_9\text{S}_8]$, chalcopyrite (CuFeS_2), bournite (Cu_5FeS_4), or pyrite (FeS_2) exhibited any evidence of reactions like 6, 7, and 8. The recovered solutions were colorless, and no dinonyl trisulfide was detected. It, thus, appears reasonable to conclude that the other sulfides did not dissociate and reactions promoted by these mineral sulfides were surface catalyzed.

3.4. Relevance of Transition Metal Sulfides to Prebiotic Metabolic Chemistry

Elucidating the possible origins of carbon fixation and anabolic chemistry is a crucial “mile-marker” on the path to understanding the origins of the phenomenon of life. Initially, the primitive Earth must have provided natural catalysts to promote the initial carbon fixation reactions, prior to the development of peptide enzymes (Wächtershäuser, 1988a, b; de Duve, 1991; Russell and Hall, 1997; Russell et al., 1998). It appears reasonable then to consider whether the reactions described above could connect with recognizable extant carbon fixation pathways, such as those utilized by primitive chemoautotrophic prokaryotes.

In the extant biological world, numerous microorganisms have evolved efficient, catalytic, methods to extract energy and synthesize biomolecules exploiting the natural thermodynamic disequilibrium of coexisting CO_2 and H_2 in crustal-derived fluids. The recent description of hydrogen-based subsurface microbial ecosystems located in continental hot springs is an excellent example of the microbial capacity to exploit this chemical potential (Chappelle et al., 2002). The organisms identified in that study evidently thrive in fluids wherein there is essentially no allochthonous organic carbon and are, therefore, true autotrophs in the sense that they synthesize their “food” directly via the reduction of CO_2 . A genomic survey of the microbial community in these hot springs revealed a predominance of Methanogenic Archaea. These are primitive organisms close to the root of molecular phylogenetic trees as constructed through sequence comparison of 16s ribosomal RNA (Woese et al., 1990). Methanogenic Archaea utilize the

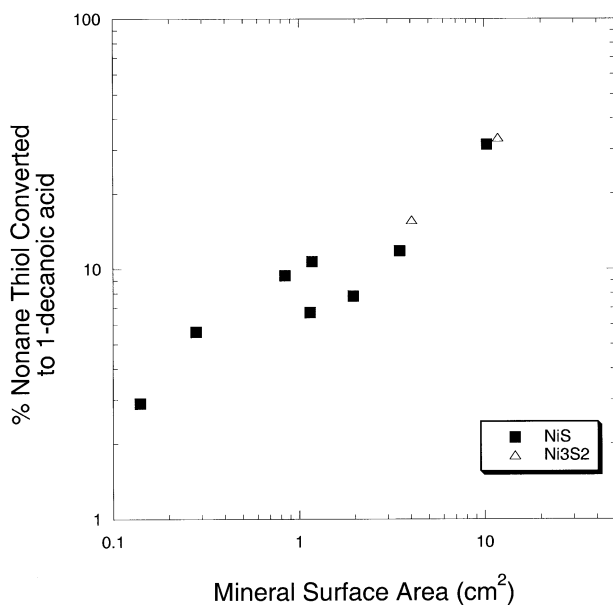


Fig. 8. Percentage of nonane thiol converted to decanoic acid as a function of metal sulfide surface area (NiS and Ni_3S_2). Conditions were 200 MPa, 250°C, and 6 h.

acetyl-CoA metabolic pathway both to fix carbon as well as to synthesize adenosine triphosphate (ATP) initially employing reactions that grossly mimic the principal reactions described above for the transition metal sulfide catalyzed reactions. It is noteworthy that recent considerations on the early evolution of autotrophy have concluded that the acetyl-CoA pathway (also known as the Wood-Ljungdahl pathway) appears to be more ancient (Peretó et al., 1999) than all other known extant autotrophic carbon fixation pathways, e.g., the reductive citrate cycle.

The first critical step in the acetyl-CoA metabolic pathway involves the production of the thioester, acetyl-CoA, a step that constitutes the threshold for all subsequent anabolic syntheses (Lengeler et al., 1999). Schematically, the formation of a thioester such as found in acetyl-CoA from CO₂, H₂, and H₂S bearing fluids can be written as



where in this reaction the product, methyl thioacetate, models the more complex acetyl-CoA thioester. Although Eqn. 9 outlines chemistry that is relatively simple in its goal, the detailed mechanism by which methanogens perform this reaction is complex. Not surprisingly, numerous enzyme catalysts are required to effect the entire process in vivo (Lengeler et al., 1999).

The acetyl-CoA synthase enzyme complex has been extensively studied in a variety of organisms, and in particular in the acetogenic bacterium, *Moorella thermoacetica* (formerly known as *Clostridia thermoacetica*; see, for example, Lindahl et al., 1990; Qiu et al., 1994). Note that, although acetogenic bacteria and methanogenic archaea lie within different domains of the prokaryotic phylogenetic tree, there remains considerable similarity in the enzyme complex that both types of organisms use to synthesize acetyl-CoA (Lengeler et al., 1999). The reaction pathways within the overall acetyl-CoA synthase enzyme complex are sketched in Figure 9. The essential feature of the complex is a pair of reaction branches, one leading to the progressive reduction of CO₂, ultimately to a transferable methyl group, whereas a second branch promotes the reduction of CO₂ to CO via a biological equivalent of the water-gas-shift-reaction (WGSR) at reaction center "C" (Fig. 9). It should be noted that recent crystallographic refinement of reaction center "C" by Dobbeck et al. (2001) revealed an Ni-4Fe-5S structure that differs slightly from that shown in Figure 9.

The two reaction branches join at the point where a methyl group (CH₃) is transferred, first to a cobalt center in a cofactor (cobalamin) and ultimately to a nickel atom in a Ni-X-Fe₄S₄ cluster; where X may be sulfur (Qiu et al., 1994). A key step in the reaction scheme involves the carbonyl insertion reaction that occurs at the Ni-X-Fe₄S₄ cluster of reaction center "A" (Fig. 9), yielding the transferable acyl group on the nickel atom (Qiu et al., 1994). Transfer of this acyl group, first to a neighboring cysteine and then to the thiol end-group of acetyl CoASH, completes the catalytic pathway (Lindahl et al., 1990).

Very recently it has been reported that an additional transition metal resides in the "A" site of acetyl Co-A synthase (Fig. 9) (Doukov et al., 2002). Electron density maps obtained from high resolution protein X-ray crystallography (2.2 angstrom

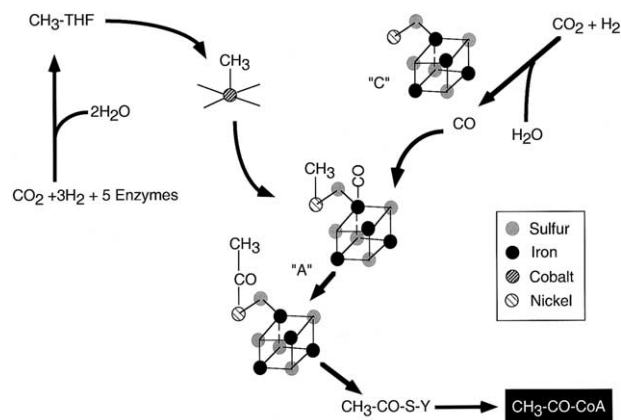


Fig. 9. Schematic representation of the active sites of acetyl-CoA synthase. The left reaction branch sequentially reduces CO₂ to a tetrahydrofolate (THF) bound methyl group. This methyl group is transferred to a cobalt cobalamin cofactor and then to a Ni-X-Fe₄S₄ cluster ("A"). The right reaction branch promotes the water-gas shift reaction reducing CO₂ to CO by utilizing a second Ni-X-Fe₄S₄ cluster ("C"). The CO carbonylates cluster "A" (initially thought to be at the iron as drawn, but more recent crystallographic data disputes this, see text). Carbonyl migration and insertion between the Ni-CH₃ bond yields the acetyl group. Transfer of the acetyl group first to a neighboring cysteine and then to the thiol end of cofactor A yields acetyl-CoA.

resolution) suggest that the "A" site actually has the configuration [Fe₄S₄]-X-M₁-X-M₂ (where M_{1,2} are transition metals and X is likely to be sulfur). Use of multiple wavelength X-ray dispersion experiments led to the conclusion that M₁ = Cu, and M₂ = Ni. Doukov et al. (2002) further propose that the Cu(I) metal is the site of acetyl formation rather than at the nickel center.

The presence of copper (I) in a critical enzyme used by a strict anaerobe is surprising as copper is typically found in enzymes that serve a protective function, e.g. radical scavenging by copper oxidases, or as cross linkers, e.g., in the synthesis of extracellular filaments in eukaryotic organisms. The correlation between previously recognized copper use in enzymes and their protective role (particularly in presence of O₂) has lead some to suggest that earliest life might not have contained any copper-bearing proteins (e.g., Fraústo da Silva and Williams, 1991). The results of Doukov et al. (2002) suggest, however, that it may be that copper is more prevalent than previously thought in enzymes of anaerobic chemoautotrophic organisms. The assay results presented above (Figs. 3, 5, and 7) reveal that chalcocite (Cu₂S) and bournite (Cu₅FeS₄), both containing univalent copper, provide apparent catalytic functionality for each of the reactions observed and are particularly effective for CO reduction and dinonyl-sulfide synthesis.

Prior to the development of enzyme catalysts, nonbiological, perhaps mineral, catalysts presumably played a critical role in carbon fixation (see, for example, the discussions in Brack, 1998). Transition metals such as Fe, Co, and Ni (and perhaps Cu; Doukov et al., 2002) play a critical role in the metabolic strategies of many of the primitive chemoautotrophic prokaryotes, as typified in acetyl-CoA synthase (Fig. 9). Other examples of enzymes that rely on transition metals and sulfur include utilization of Mo and Fe in the nitrogenases (Howard and Rees, 1996); Fe and Ni in hydrogenases (Cammack, 1988);

and W and Mo in aldehyde oxidoreductase enzymes (Kletzin and Adams, 1996).

Many of the transition metals required in prokaryotic enzymes have low average abundance in the Earth's crust (Lederer and Shirley, 1978). If prebiotic carbon fixation arose utilizing minerals containing a high abundance of such elements, then it would appear advantageous for such processes to have arisen in environments naturally endowed with an abundance of such elements. Volcanic associated massive sulfide (VMS) deposits and associated hot springs may have provided particularly favorable environments as well as fluids containing H_2 and CO_2 (e.g., Holm, 1992; Russell et al., 1998). It is interesting to note that abiogenic hydrocarbons (methane, ethane, propane, and butane) are detected in bore-holes penetrating the 2.7 Ga Kidd Creek VMS deposit in Ontario, Canada (Sherwood Lollar et al., 2002). It is likely that these hydrocarbons formed via FT processes catalyzed by the abundance of transition metal sulfides present in the deposit.

The experiments described above demonstrate the capacity of transition metal sulfides to promote many of the reactions manifest in the more complex acetyl-CoA metabolic pathway. For example, comparing these results with acetyl-CoA pathway (Fig. 9) it is seen that the branch involving the reduction of CO_2 to a transferable CH_3 group is performed readily by all of the mineral sulfides assayed in this study (Fig. 5); with Cu_2S , FeS, and CuS being particularly effective in this process. Furthermore, the carbonyl insertion reaction at the coalescence of the two reaction branches or acetyl-CoA synthase depicted in Figure 9, is also readily promoted by almost all of the transition metal sulfides assayed here (Fig. 3).

4. CONCLUSIONS

The experiments described above, as well as those of others (Heinen and Lauwers, 1996; Huber and Wächtershäuser, 1997; Cody et al., 2000, 2001), highlight the properties of transition metal sulfides in promoting potentially useful prebiotic chemistry. The following observations can be made. First, based on the current experiments there is evidence that the reactions are being surface catalyzed. Surface catalysis was presumably required prebiotically under dilute natural conditions. Second, each of the metal sulfides studied exhibited at least some form of catalytic activity under the prevailing reaction conditions. Although the range of naturally occurring sulfides (as well as compositional variation within each mineral group) far exceed the modest suite of pure metal sulfides studied here, the present results suggest that one may not need to invoke a special composition or particular mineral phase in order to access useful catalytic qualities. Finally, comparison of the relative selectivity for different reactions among the sulfides studied, e.g., CuS vs. Ni_3S_2 , indicates that studies of consortia of metal sulfides may reveal interesting synergistic or antagonistic effects.

It is reasonable to consider how far such chemistry could go in promoting useful and/or necessary prebiotic organic chemistry. Recently, Cody et al. (2001) demonstrated experimentally that metal sulfide catalysis could promote a series of hydrocarboxylation reactions highlighting a potential reaction pathway leading up from propene to hydroaconitic acid; i.e., an abiotic carbon fixation pathway that ends one oxygen atom away from

citric acid. The potential utility of such a pathway lies in the fact that it is well known that under hydrothermal conditions citric acid is a prolific source of pyruvic acid (Carlsson et al., 1994; Cody et al., 2001). Pyruvic acid is a very useful prebiotic product, for example, in the presence of NH_4^+ a simple reductive amination reaction provides a ready source of alanine (Brandes et al., 1999). Along a separate pathway, starting with alkane thiols and CO, it has also been shown that reactions over FeS can lead to the synthesis of alpha ketoacids, including pyruvic acid (Cody et al., 2000).

How then do these results add to the debate between hot and cold origins of life? First, it must be stressed that the present experiments were not designed to directly explore the origins of life, rather they were designed and optimized to assay the catalytic activity of metal sulfides to promote chemistry of possible relevance to the origins of life inquiries. Consequently, the present results should not be misinterpreted as providing direct support that life could have arisen at temperatures as high as $250^\circ C$. In fact, the present results suggest quite the opposite. For example, one compound that would be important to the origins of biochemistry, nonyl thiodecanoate (a thioester), was not observed in the present experiments. Huber and Wächtershäuser (1997), on the other hand, reported the synthesis of methyl thioacetate in their experiments at a considerably lower temperature ($100^\circ C$).

In the present experiments thioesters should readily form by the transfer of a decanoyl group to either a methane thiol or nonane thiol. As evident in the data shown in Figure 7, there is extensive evidence of interaction of nonane thiol with metal bound nonyl groups resulting in high yields of dinonyl sulfide. It is also likely, therefore, that nonane thiol would also react with metal-bound decanoyl groups to yield the thioesters. The experimental conditions, however, were chosen to provide an optimum assay of the transition metal sulfides by enhancing turnover rates via the accelerated hydrolysis of metal bound decanoyl groups. Such experimental conditions will severely limit the accumulation of thermally labile thioesters by promoting the rapid hydrolysis of any thioester formed to yield carboxylic acid and alkane thiol. The lack of detectable thioesters detected in the current experiments, as compared with the significant abundance of methyl thioester detected by Huber and Wächtershäuser (1997), is therefore, likely due to the higher temperatures employed in this study, rather than differences in catalytic quality of the phases used in each study.

There clearly must be an upper temperature limit for the emergence of the phenomenon of life to be feasible. Certainly $250^\circ C$ is too hot if thioesters are required as intermediates for prebiotic organosynthesis (e.g., de Duve, 1991). This limit stands regardless that other useful carbon fixation reactions can be shown to occur at such high temperatures (e.g., Cody et al., 2000, 2001). The central problem is that many important biomolecules are thermally unstable in aqueous media; e.g., functionalized sugars (both aminated and phosphorylated), peptides, polyphosphates, and thioesters will not survive long in water under hot hydrothermal conditions (see for example, Larralde et al., 1995; Shapiro, 1995). Nitriles, such as cyanoacetylene and cyanoacetaldehyde (proposed as possible prebiotic precursors for pyrimidines; Robertson and Miller, 1995), will be rapidly hydrolyzed to carboxylic acids in hot water (Siskin et al., 1990). Therefore, if the synthesis of nucleotides and their

subsequent oligomerization to promote an “RNA” world is requisite to the emergence of life, then such chemistry would be extremely improbable (if not impossible) in high-temperature water (see, for example, Miller and Lazcano, 1995).

In a preenzymatic world, mineral catalysts were undoubtedly required to initiate a broad range of organosynthetic reactions that produced the first biomolecules driven by the chemical potential available within the natural abiotic environment. For at least some of this chemistry, it is difficult to conceive of better, naturally occurring, prebiotic catalysts than metal sulfides. The challenge remains to demonstrate which catalysts did what and where the prebiotic chemistry ultimately converged into the phenomenon of life itself. The results of the experiments described above indicate that cool environments in close proximity to metal sulfide precipitating hydrothermal hot springs may have been advantageous to the emergence of life on the early Earth.

Acknowledgments—This research was carried out under the auspices of the NASA Astrobiology Institute under NASA Cooperative Agreement NCC2-1056. The authors gratefully acknowledge stimulating discussions with Drs. Marilyn Fogel, Ken Nealson, S. Nick Platts, James Scott, and Anurag Sharma. This manuscript benefited from thoughtful reviews by Michael Russell and two anonymous reviewers.

Associate editor: P. A. O’Day

REFERENCES

- Abel E. W. and Crosse B. C. (1967) Sulfur-containing metal carbonyls. *Organometal. Chem. Rev.* **2**, 443–494.
- Abeles R. H., Frey P. A., and Jencks W. P. (1992) *Biochemistry*. Jones and Bartlet.
- Adamson A. W. (1990) *Physical Chemistry of Surfaces*. Wiley.
- Bain C. D., Troughton E. B., Tao Y.-T., Evall J., Whitesides G. M., and Nuzzo R. G. (1989) Formation of monolayer films by spontaneous assembly of organic thiols from solution on gold. *J. Am. Chem. Soc.* **111**, 321–335.
- Blau K. and King G. S., eds. (1977) *Handbook of Derivatives for Chromatography*. Hedyen Bellmaw.
- Brack A., ed. (1998) *The Molecular Origins of Life*. Cambridge University Press.
- Boudart M. and Djéga-Mariadassou G. (1984) *Kinetics of Heterogeneous Catalytic Reactions*. Princeton University Press.
- Brandes J. A., Boctor N. Z., Hazen R. M., Yoder H. S. Jr., and Cody G. D. (1999) Prebiotic amino acid synthesis pathways via α -keto acids: An alternative to the Strecker synthesis. In *Perspectives in Amino Acid and Protein Geochemistry* (eds. G. A. Goodfriend, M. J. Collins, M. L. Fogel, S. A. Macko, and J. F. Wehmiller). pp. 41–47. Oxford University Press.
- Cammack R. (1988) Nickel in metalloproteins. *Adv. Org. Chem.* **32**, 297–333.
- Carlsson M., Habenicht C., Kam L. C., Antal M. J., Jr., Bian H., Cunningham R. J., and Jones M., Jr. (1994) Study of the sequential conversion of citric to itaconic acid to methylacrylic acid in near-critical and supercritical water. *Ind. Eng. Chem. Res.* **33**, 1989–1996.
- Chappelle F. H., O’Neill K., Bradley P. M., Methé B. A., Ciufo S. A., Knobel L. L., and Lovely D. R. (2002) A hydrogen-based subsurface microbial community dominated by methanogens. *Nature* **413**, 312–315.
- Cody G. D., Boctor N. Z., Filley T. R., Hazen R. M., Scott J. H. A., and Yoder H. S., Jr. (2000) The primordial synthesis of carbonylated iron-sulfur clusters and the synthesis of pyruvate. *Science* **289**, 1339–1341.
- Cody G. D., Boctor N. Z., Hazen R. M., Brandes J. A., Morowitz H. J., and Yoder H. S., Jr. (2001) Geochemical roots of autotrophic carbon fixation: Hydrothermal experiments in the system citric acid-H₂O-(\pm FeS)-(\pm NiS). *Geochim. Cosmochim. Acta* **65**, 3557–3576.
- Cotton F. A. and Wilkinson G. (1988) *Advanced Inorganic Chemistry*. Wiley.
- Crabtree R. H. (1997) Where smokers rule. *Science* **276**, 222–223.
- de Duve C. (1991) *Blueprint for a Cell*. Neil Patterson.
- Dobbeck K. H., Svetlitchnyi V., Gremer L., Huber R., and Meyer O. (2001) Crystal structure of a carbon monoxide dehydrogenase reveals a [Ni-4Fe-5S] cluster. *Science* **293**, 1281–1285.
- Doukov T. I., Iverson T. M., Seravalli J., Ragsdale S. W., and Drennen C. L. (2002) A Ni-Fe-Cu center in a bifunctional carbon monoxide dehydrogenase/acetyl-CoA synthase. *Science* **298**, 567–571.
- Fischer F. (1935) Die Synthese der Treibstoffe (Kogain) und Schmieröle aus Kohlenoxyd und Wasserstoff bei gewöhnlichem Druck. *Brennstoff-Chemie* **16**, 1–11.
- Fraústo da Silva J. J. R. and Williams R. J. P. (1991) *The Biological Chemistry of the Elements*. Clarendon Press.
- Guevremont J. M., Elsetinow A. R., Strongin D. R., Bebié J., and Schoonen M. A. A. (1998) Structure sensitivity of pyrite oxidation: Comparison of the (100) and (111) planes. *Am. Mineral.* **83**, 1353–1356.
- Hall A. J. (1986) Pyrite-pyrrhotine redox reactions in nature. *Min. Mag.* **50**, 223–229.
- Hayatsu R. and Anders E. (1981) Organic compounds in meteorites and their origins. *Topics Curr. Chem.* **99**, 1–37.
- Heinen W. and Lauwers A. M. (1996) Organic sulfur compounds resulting from the interaction of iron sulfide, hydrogen sulfide and carbon dioxide in an aerobic aqueous environment. *Origins Life Evol. Biosphere* **26**, 131–150.
- Holm N. G., ed. (1992) *Marine Hydrothermal Systems and the Origin of Life*. Kluwer Academic Publishers.
- Howard J. B. and Rees D. C. (1996) Structural basis for nitrogen fixation. *Chem. Rev.* **96**, 2952–2982.
- Huber C. and Wächtershäuser G. (1997) Activated acetic acid by carbon fixation on (Fe,Ni)S under primordial conditions. *Science* **276**, 245–247.
- Kletzin A. and Adams M. W. W. (1996) Tungsten in biology. *FEMS Microbiol. Rev.* **18**, 5–64.
- Kress M. E. and Tielens S. (2001) The role of Fischer-Tropsch catalysis in solar-nebula chemistry. *Meteor. Planet. Sci.* **36**, 75–82.
- Kullerød G. (1971) *Research Techniques for High Pressure and Temperature*. Springer-Verlag.
- Larralde R., Robertson M. P., and Miller S. L. (1995) Rates of decomposition of ribose and other sugars: Implications for chemical evolution. *Proc. Natl. Acad. Sci. USA* **92**, 8158–8160.
- Lederer C. M. and Shirley V. S. (1978) *Table of Isotopes*. 7th ed. Wiley.
- Lengeler J. W., Drews G., and Schlegel H. G. (1999) *Biology of the Prokaryotes*. Blackwell Science.
- Lindahl P. A., Münck E., and Ragsdale S. W. (1990) CO dehydrogenase from *Clostridium thermoaceticum*. *J. Biol. Chem.* **265**, 3873–3879.
- March J. (1991) *Advanced Organic Chemistry*. Wiley.
- McCollom T. M., Ritter G., and Simoneit B. R. (1999) Lipid synthesis under hydrothermal conditions by Fischer-Tropsch-type reactions. *Origins Life Evol. Biosphere* **29**, 153–166.
- Miller S. L. and Lazcano A. (1995) The origin of life—Did it occur at high temperatures? *J. Mol. Evol.* **41**, 689–692.
- Peretó J. G., Velasco A. M., Becerra A., and Lazcano A. (1999) Comparative biochemistry of CO₂ fixation and the evolution of autotrophy. *Int. Microbiol.* **2**, 3–10.
- Qiu D., Kumar M., Ragsdale S. W., and Spiro T. G. (1994) Nature’s carbonylation catalyst: Raman spectroscopic evidence that carbon monoxide binds to iron, not nickel, in CO dehydrogenase. *Science* **264**, 817–819.
- Robertson M. P. and Miller S. L. (1995) An efficient prebiotic synthesis of cytosine and uracil. *Nature* **375**, 772–774.
- Russell M. J. and Hall A. J. (1997) The emergence of life from iron monosulfide bubbles at a submarine hydrothermal redox and pH front. *J. Geol. Soc. Lond.* **154**, 377–402.
- Russell M. J., Daia D. E., and Hall A. J. (1998) The emergence of life from FeS bubbles at alkaline hot springs in an acid ocean. In *Thermophiles: The Keys to Molecular Evolution and the Origin of*

- Life?* (eds. J. Wiegel and M. W. W. Adams), pp. 77–126. Taylor and Francis.
- Schoonen M. A. A., Xu Y., and Strongin D. R. (1998) An introduction to geocatalysis. *J. Geochem. Exp.* **62**, 201–215.
- Schulte M. D. and Shock E. L. (1993) Aldehydes in hydrothermal solutions: Standard partial molal thermodynamic properties and relative stabilities at high temperatures and pressures. *Geochim. Cosmochim. Acta* **57**, 3835–3846.
- Shapiro R. (1995) The prebiotic role of adenine: a critical analysis. *Origins Life Evol. Biosphere* **25**, 83–98.
- Sherwood Lollar B., Westgate T. D., Ward J. A., Slater G. F., and Lacrampe-Couloume G. (2002) Abiogenic formation of alkanes in the Earth's crust as a minor source for global hydrocarbon reservoirs. *Nature* **416**, 522–524.
- Shock E. L. (1992) Chemical environments of submarine hydrothermal systems. *Origins Life Evol. Biosphere* **22**, 67–107.
- Shock E. L., McCollum T., and Schulte M. D. (1996) Geochemical constraints on chemolithoautotrophic reactions in hydrothermal systems. *Origins Life Evol. Biosphere* **25**, 141–159.
- Siskin M., Brons G., Katritzky A. R., and Balasubramanian M. (1990) Aqueous organic chemistry. 1. Aquathermolysis: Comparison with thermolysis in the reactivity of aliphatic compounds. *Energy Fuels* **4**, 475–492.
- Steinfeld J. I., Francisco J. S., and Hase W. L. (1989) *Chemical Kinetics and Dynamics*. Prentice-Hall.
- Tivey M. K. (1995) The influence of hydrothermal fluid composition and advection rates on black smoker chimney mineralogy: Insights from modeling transport and reaction. *Geochim. Cosmochim. Acta* **59**, 1933–1949.
- Wächtershäuser G. (1988a) Before enzymes and templates: Theory of surface metabolism. *Microbiol. Rev.* **52**, 452–484.
- Wächtershäuser G. (1988b) Pyrite formation, the first energy source for life: A hypothesis. *System. Appl. Microbiol.* **10**, 207–210.
- Woese C., Kandler O., and Wheelis M. (1990) Towards a natural system of organisms: Proposal for the domains Archaea, Bacteria, and Eucarya. *Proc. Natl. Acad. Sci USA* **87**, 4576–4579.
- Yoder H., Jr. (1950) High-low quartz inversion up to 10,000 bars. *Trans. Am. Geophys. Union* **31**, 821–835.

Appendix. Electron impact mass fragmentation data of principal products.

Compound	MW	Fragmentation ^a
1-Decanoic acid, propyl ester	214	214(5,M);173(65,M-CH ₂ CHCH ₂);155(50,M-CH ₃ CH ₂ CH ₂ O);143(5);129(23);115(25);102(35);87(10);73(40); 61(100)* ;55(35);43(65)
2-Methylnonanoic acid, propyl ester	214	214(3,M);173(45);155(20);143(5);129(15);116(70);101(5)87(30); 74(100) ;57(25);43(60)
2-Ethyl octanoic acid, propyl ester	214	214(3,M);173(60);155(30);143(20);130(85);115(20);101(40); 88(100) ;73(55);55(45);43(85)
2-Propylheptanoic acid, propyl ester	214	214(1,M);173(60);155(30);144(65);130(25);115(90);102(35);85(20); 73(100) ;55(45);43(85)
2-Butylhexanoic acid, propyl ester	214	214(1,M);173(50);158(80);155(25);143(5);129(33);115(90);101(1);85(25); 73(100) ;55(60);43(85)
1-Undecanoic acid, propyl ester	228	228(5,M);187(45, M-CH ₂ CHCH ₂);169(35, M-CH ₃ CH ₂ CH ₂ O);157(5);143(10);129(15);115(20);102(30);87(15);73(40); 61(100) ;55(35);43(55)
3-Methyldecanoic acid, propyl ester	228	228(2,M);187(45);169(20);157(2);143(10);129(20);116(85);101(5);87(35); 74(100) ;57(30);43(60)
3-Ethylnonanoic acid, propyl ester	228	187(60);169(20);157(10);143(15);130(95);115(20);101(35); 88(100) ;73(50);57(45);43(80)
3-Propyl octanoic acid, propyl ester	228	187(50);169(25);157(20);144(80);129(10); 115(100) ;102(35);85(20);73(95);55(60);43(80)
3-Butylheptanoic acid, propyl ester	228	187(35);169(35);158(70);143(15);130(30);115(70);85(15); 73(100) ;57(25);43(25)
1-Dodecanoic acid, propyl ester	242	242(5,M);202(40,M-CH ₂ CHCH ₂);183(35,M-CH ₃ CH ₂ CH ₂ O); 171(10);157(10);143(5);129(12);115(30);102(35);83(12);73(40); 61(100) ;55(35);43(60)
4-Methylundecanoic acid, propyl ester	242	201(20);183(25);131(20);115(65);102(30);85(25);73(75);61(85);57(55); 43(100)
4-Ethyldecanoic acid, propyl ester	242	201(35);183(25);143(10);129(20); 116(100) ;101(5);87(35);74(98);57(40);43(75)
4-Propylnonanoic acid, propyl ester	242	202(35);183(20);173(25);155(25);130(65);115(20);101(25);88(60);71(50);61(45);57(70); 43(100)
2-Pentylthiophene	154	154(25,M);111(8); 97(100,CH₂-thiophene⁺)
Methyl undecanoate	200	200(20,M);87(20); 74(100)
1-Methylthio-2-thiononane	206	206(60,M);85(50);80(40);71(95); 57(100)
Dinonyl sulfide	286	286(15,M);173(8,nonyl-S-CH ₂ +); 159(100,nonyl-S⁺) ;126(15,nonyl-H ⁺);155(5);97(20);83(30);69(45);61(25);55(55)
1,2-Dinonyl sulfide	286	286(20,M); 187(100,nonyl-S-CH₂CH₂+) ;159(98,nonyl-S ⁺);126(25);97(35);83(55);75(33);69(85);61(25);55(55)
Nonyl decyl sulfide	300	300(20,M);173(90,decyl-S ⁺);159(85,nonyl-S ⁺);140(12,decyl-H ⁺);126(15,nonyl-H ⁺);97(35);83(60);69(70);61(50); 55(100)
Dinonyl disulfide	318	318(25,M);192(20,nonyl-S ₂ -H ⁺);159(25,nonyl-S ⁺);129(5);115(8);101(10);85(60);71(95); 57(100)
Nonyl decyl disulfide	332	332(25,M);208(20,decyl-S ₂ -H ⁺);192(13,nonyl-S ₂ -H ⁺);173(15,decyl-S ⁺);159(15,nonyl-S ⁺);115(10);85(55);71(75); 57(100)
1-Nonylthio-2-methylthiononane	332	332(20,M);201(18);173(80,nonyl-S-CH ₂ +);159(30);157(33,CH ₃ (CH ₂) ₆ CHCH ₃ +);124(18);115(16);101(20);83(60); 69(100) ;61(100);57(80)
Dinonyl trisulfide	350	350(40,M);285(8);224(5,nonyl-S ₃ -H ⁺);192(12,nonyl-S ₂ -H ⁺);159(nonyl-S ⁺);129(5);115(12);101(18);85(45);71(80); 57(100)
1-Nonylthio-2-propylthiononane	360	360(5,M); 201(100,M-nonyl-S) ;157(3);129(1);115(3);101(5);89(30);69(28);55(25)

^a Fragment mass *m/z*, percentage intensity relative to base peak (base peak ions presented in bold); M = molecular weight.